

Electronic Supplementary Information (ESI)

Channel confinement and separation properties in an adaptive supramolecular framework using an adamantane tecton

Nicholas Lutz, Josephine Bicknell, Jesus Daniel Loya, Eric W. Reinheimer, and Gonzalo Campillo-Alvarado*

Department of Chemistry, Reed College, Portland, OR 97202, USA.

*e-mail: gcampillo@reed.edu

Supplementary Information:

- S1) Experimental information
- S2) Single-crystal X-ray data
- S3) Non-covalent interactions table
- S4) NMR spectral data
- S5) UNI force field calculations

S1. Experimental information

Materials:

1,3,5,7-tetrakis(4-bromophenyl)adamantane (**1**) was obtained from Combi-Blocks. Solvents benzene (**C₆H₆**) and toluene (**tol**) were obtained from Sigma-Aldrich. Solvent chloroform (**CHCl₃**) was obtained from JT Baker. Solvent dichloromethane (**dcm**) was obtained from Macron. Solvent *p*-xylene (***p*-xyl**) was obtained from TCI. All reagents and solvent were used as received.

Single crystals of (**1**)·(**C₆H₆**) were generated by dissolving **1** (19.8 mg, 0.026 mmol) in **C₆H₆** (2.5 mL) and gently heating until complete dissolution. Single crystals of (**1**)·(**CHCl₃**) were generated by dissolving **1** (17.9 mg, 0.024 mmol) in **CHCl₃** (2.5 mL), no heat was required for complete dissolution. Single crystals of (**1**)·(***p*-xyl**) were generated by dissolving **1** (15.2 mg, 0.020 mmol) in ***p*-xyl** (2.5 mL), no heat was required for complete dissolution. Single crystals of (**1**)·(**tol**) were generated by dissolving **1** (17.9 mg, 0.024 μmol) in **tol** (2.5 mL) and gently heated until complete dissolution. Single crystals were formed from each solution after a 2-4 day period. Single crystals of **apo-1** were generated by dissolving **1** (15.8 mg, 20.89 μmol) in **dcm** (2.5 mL) and following the procedure above for solvates, no heat should be required for complete dissolution in **dcm**.

Instruments and methods:

¹H NMR spectra were recorded on a Bruker AV400 spectrometer with chloroform-*d* (7.26 ppm) and DMSO-*d*₆ (2.50 ppm) as internal standards. IR spectra were recorded on a Thermo Scientific Nicolet iS5 FT-IR spectrometer with an iD5 ATR accessory. NMR data was processed with Mnova suite, and IR data was processed with OMNIC™ Software and RStudio software. Single crystal X-ray diffraction (SCXRD) data was collected on a Rigaku XtaLAB Mini II diffractometer with a CCD area detector (λMoKα = 0.71073 Å, monochromator: graphite). Experiments were conducted at 100 K with a range of 2θ = 3-62°. The collected data was refined with CrysAlisPro through standard data reduction and background corrections (analytical for **apo-1**, (**1**)·(**CHCl₃**), (**1**)·(**tol**), and multi-scan for (**1**)·(**CHCl₃**), (**1**)·(***p*-xyl**)). Crystals were mounted in Paratone oil on a Mitegen magnetic mount. Structure solution and refinement were performed using SHELXT¹ and SHELXL,² respectively within the Olex2³ and WinGX⁴ graphical user interfaces.

Separation of **C₆H₆** and **tol** was performed by dissolving **1** (15.4 mg, 0.020 mmol) in 2.5 mL of solution of a 1:1 (v/v) binary mixture of the solvents. The resulting crystals (3-4 days of slow evaporation) were rapidly filtered, dried, and analyzed by ¹H NMR spectroscopy. To carry out repeated solvent uptake, a solution was prepared with the ratio of **C₆H₆** and **tol** observed by ¹H NMR spectroscopy from the previous batch of crystals.

S2. Single-crystal X-ray data

Table S1. Crystallographic parameters for **apo-1**

Compound name	apo-1
Empirical formula	C ₆₈ H ₅₆ Br ₈
Formula weight	1512.431
Temperature/K	100.15
Crystal system	triclinic
Space group	P-1
a/Å	10.8095(7)
b/Å	15.4233(9)
c/Å	19.8301(10)
α/°	67.615(5)
β/°	80.075(5)
γ/°	74.356(5)
Volume/Å³	2934.7(3)
Z	4
ρ_{calc}/g/cm³	1.712
μ/mm⁻¹	5.508
F(000)	1488.0
Crystal size/mm³	0.374 × 0.174 × 0.044
Radiation	Mo Kα (λ = 0.71073)
2θ range for data collection/°	3.924 to 50.246
Index ranges	-12 ≤ h ≤ 12, -18 ≤ k ≤ 18, -23 ≤ l ≤ 23
Reflections collected	39921
Independent reflections	10436 [R _{int} = 0.0676, R _{sigma} = 0.0914]
Data/restraints/parameters	10436/0/685
Goodness-of-fit on F²	1.032
Final R indexes [I ≥ 2σ (I)]	R ₁ = 0.0524, wR ₂ = 0.1061
Final R indexes [all data]	R ₁ = 0.1042, wR ₂ = 0.1219
CCDC deposition number	2289644

Table S2. Crystallographic parameters for (1)·(C₆H₆)

Compound name	(1)·(C ₆ H ₆)
Empirical formula	C _{14.5} H ₁₃ Br
Formula weight	267.16
Temperature/K	100.00(10)
Crystal system	tetragonal
Space group	P-42 ₁ c
a/Å	18.4930(7)
b/Å	18.4930(7)
c/Å	7.1799(5)
α/°	90
β/°	90
γ/°	90
Volume/Å³	2455.5(3)
Z	1
ρ_{calc}/g/cm³	1.445
μ/mm⁻¹	3.315
F(000)	1080.0
Crystal size/mm³	0.181 × 0.12 × 0.094
Radiation	Mo Kα (λ = 0.71073)
2θ range for data collection/°	4.406 to 56.726
Index ranges	-23 ≤ h ≤ 24, -19 ≤ k ≤ 24, -9 ≤ l ≤ 9
Reflections collected	12261
Independent reflections	2967 [R _{int} = 0.0616, R _{sigma} = 0.0824]
Data/restraints/parameters	2967/0/142
Goodness-of-fit on F²	1.000
Final R indexes [I >= 2σ (I)]	R ₁ = 0.0394, wR ₂ = 0.0728
Final R indexes [all data]	R ₁ = 0.0684, wR ₂ = 0.0820
CDCC deposition number	2289640

Table S3. Crystallographic parameters for (1)·(tol)

Compound name	(1)·(tol)
Empirical formula	C ₄₁ H ₃₆ Br ₄
Formula weight	848.34
Temperature/K	100.00(10)
Crystal system	monoclinic
Space group	C2
a/Å	19.2611(14)
b/Å	7.1873(7)
c/Å	25.1626(19)
α/°	90
β/°	94.187(8)
γ/°	90
Volume/Å³	3474.1(5)
Z	4
ρ_{calc}/cm³	1.622
μ/mm⁻¹	4.662
F(000)	1688.0
Crystal size/mm³	0.275 × 0.156 × 0.06
Radiation	Mo Kα (λ = 0.71073)
2θ range for data collection/°	4.87 to 50.24
Index ranges	-22 ≤ h ≤ 22, -8 ≤ k ≤ 8, -28 ≤ l ≤ 30
Reflections collected	11552
Independent reflections	11552 [R _{int} = ?, R _{sigma} = 0.0824]
Data/restraints/parameters	11552/370/410
Goodness-of-fit on F²	1.056
Final R indexes [I ≥ 2σ (I)]	R ₁ = 0.0493, wR ₂ = 0.1010
Final R indexes [all data]	R ₁ = 0.0660, wR ₂ = 0.1064
CCDC deposition number	2289643

Table S4. Crystallographic parameters for (1)·(p-xyI)

Compound name	(1)·(p-xyI)
Empirical formula	C ₄₂ H ₃₈ Br ₄
Formula weight	862.36
Temperature/K	101.15
Crystal system	monoclinic
Space group	P2 ₁
a/Å	7.1953(3)
b/Å	25.4666(9)
c/Å	10.1699(4)
α/°	90
β/°	107.729(4)
γ/°	90
Volume/Å³	1775.03(13)
Z	2
ρ_{calc}/cm³	1.613
μ/mm⁻¹	4.564
F(000)	860.0
Crystal size/mm³	0.327 × 0.183 × 0.042
Radiation	Mo Kα (λ = 0.71073)
2θ range for data collection/°	4.204 to 50.246
Index ranges	-8 ≤ h ≤ 8, -29 ≤ k ≤ 30, -12 ≤ l ≤ 12
Reflections collected	14726
Independent reflections	6146 [R _{int} = 0.0453, R _{sigma} = 0.0671]
Data/restraints/parameters	6146/1/417
Goodness-of-fit on F²	1.034
Final R indexes [I ≥ 2σ (I)]	R ₁ = 0.0374, wR ₂ = 0.0644
Final R indexes [all data]	R ₁ = 0.0458, wR ₂ = 0.0665
CCDC deposition number	2289642

Table S5. Crystallographic parameters for (1)·(CHCl₃)

Compound name	(1)·(CHCl ₃)
Empirical formula	C _{17.5} H _{14.5} Br ₂ Cl _{1.5}
Formula weight	437.79
Temperature/K	100.15
Crystal system	monoclinic
Space group	C2/c
a/Å	18.7063(12)
b/Å	7.1729(5)
c/Å	25.574(2)
α/°	90
β/°	101.643(7)
γ/°	90
Volume/Å³	3360.9(4)
Z	4
ρ_{calc}/cm³	1.730
μ/mm⁻¹	5.053
F(000)	1720.0
Crystal size/mm³	0.194 × 0.135 × 0.022
Radiation	Mo Kα (λ = 0.71073)
2θ range for data collection/°	4.952 to 50.24
Index ranges	-21 ≤ h ≤ 22, -8 ≤ k ≤ 7, -30 ≤ l ≤ 30
Reflections collected	11599
Independent reflections	2975 [R _{int} = 0.0758, R _{sigma} = 0.1008]
Data/restraints/parameters	2975/18/203
Goodness-of-fit on F²	1.058
Final R indexes [I >= 2σ (I)]	R ₁ = 0.0672, wR ₂ = 0.1635
Final R indexes [all data]	R ₁ = 0.1150, wR ₂ = 0.1851
CCDC deposition number	2289641

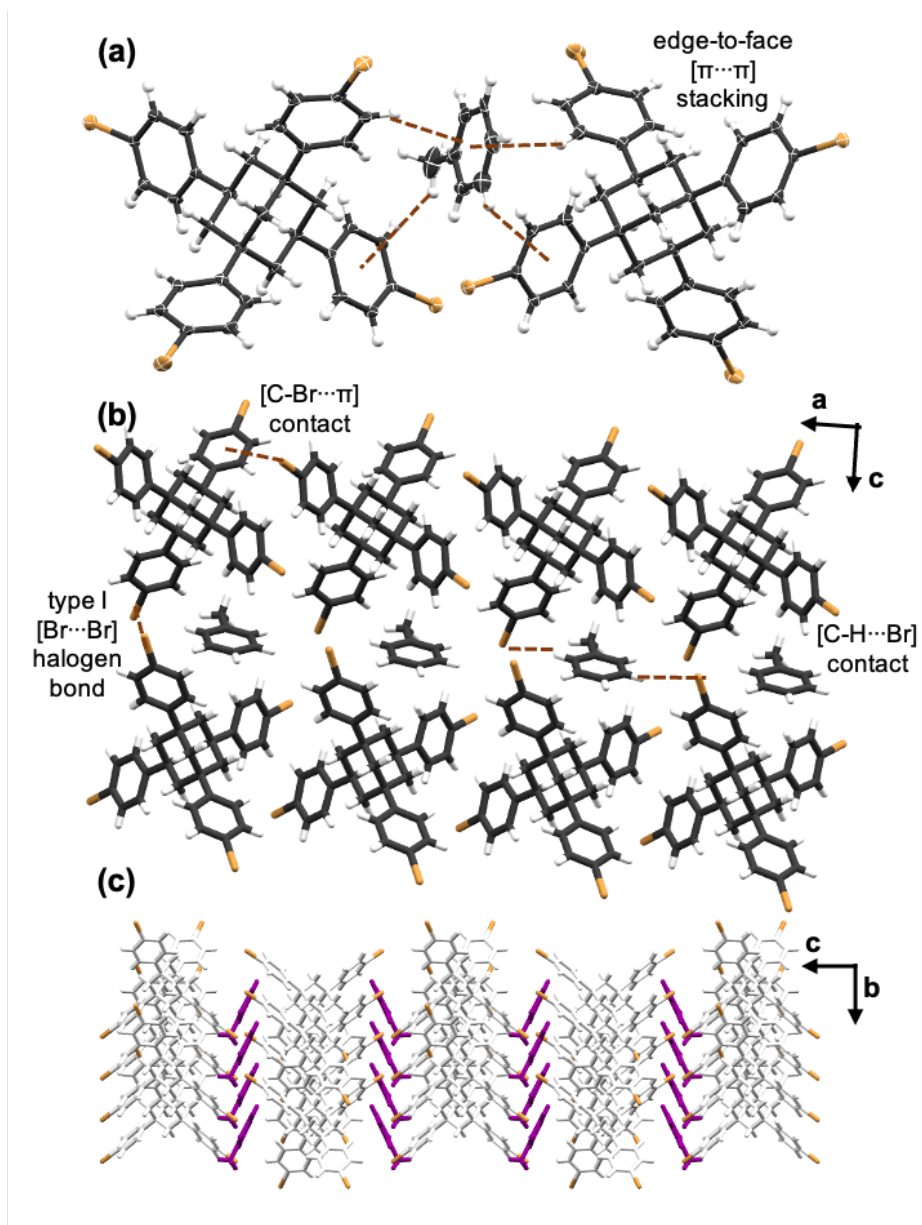


Figure S1. X-ray structure of **1**·(tol): (a) edge-to-face $[\pi \cdots \pi]$ stacking between **tol** and **1**, (b) $[\text{C}-\text{Br} \cdots \pi]$, $[\text{Br} \cdots \text{Br}]$, and $[\text{C}-\text{H} \cdots \text{Br}]$ contacts, (c) van der Waals contacts of **1** in *bc*-plane and channel formation along *b*-axis.

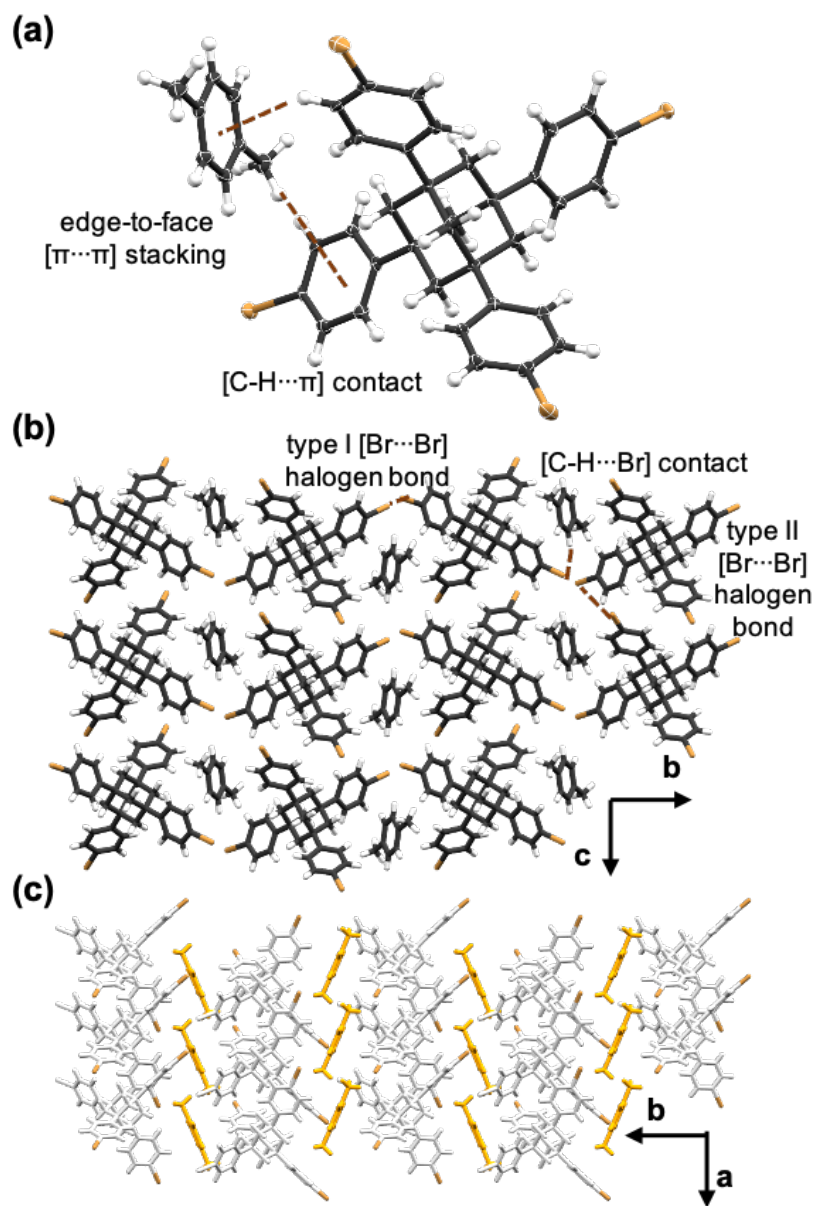


Figure S2. X-ray structure of $1 \cdot (p\text{-xyI})$: (a) edge-to-face $[\pi \cdots \pi]$ stacking and $[\text{C-H} \cdots \pi]$ contacts between $p\text{-xyI}$ and 1 , (b) $[\text{Br} \cdots \text{Br}]$ (type I and II), and $[\text{C-H} \cdots \text{Br}]$ contacts, (c) van der Waals contacts of 1 in ab -plane and channel formation along a -axis.

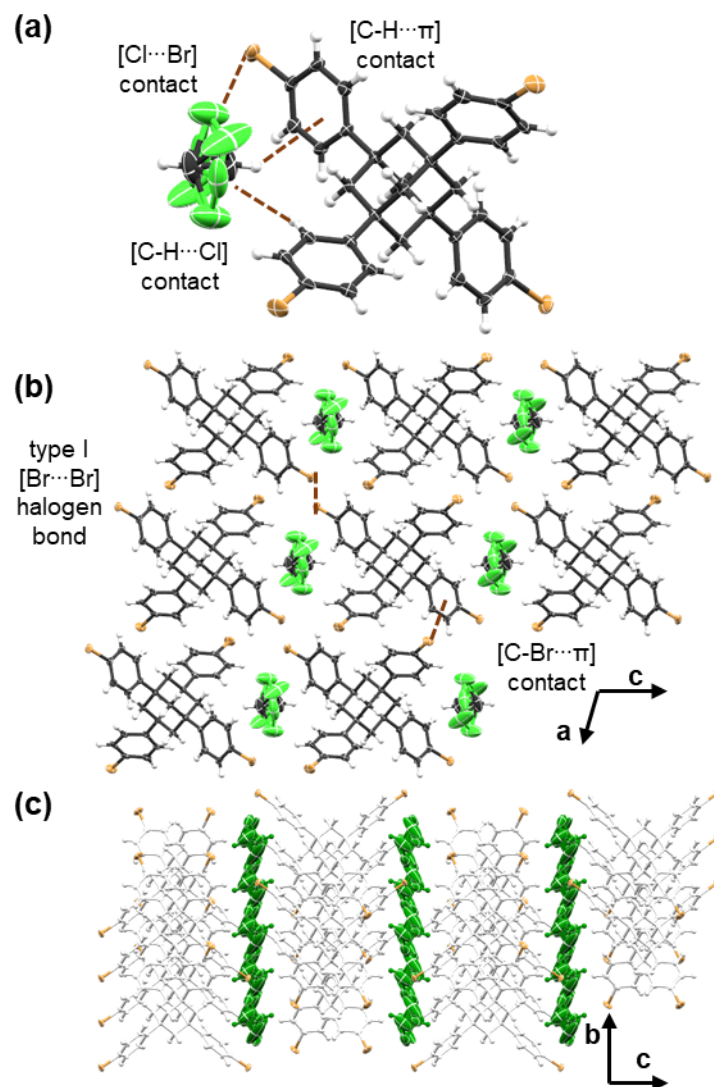


Figure S3. X-ray structure of $1 \cdot (\text{CHCl}_3)$: (a) $[\text{Cl} \cdots \text{Br}]$, $[\text{C-H} \cdots \pi]$, and $[\text{C-H} \cdots \text{Cl}]$ contacts between CHCl_3 and **1**, (b) $[\text{Br} \cdots \text{Br}]$ (type I), and $[\text{C-Br} \cdots \pi]$ contacts, (c) van der Waals contacts of **1** in bc -plane and channel formation along b -axis.

Table S6. Selected intermolecular interactions in crystals

Crystal/parameter	$d(\text{C}\cdots\text{X})$ (Å)	$d(\text{X}\cdots\text{X})$ (Å)	$d(\text{C-H}\cdots\pi)$	symmetry code
apo-1	3.708(6) ¹	-	-	(1+X, +Y, +Z)
	-	-	2.965(2) ²	
1·(C ₆ H ₆)	3.530 (5) ³	-	-	(-1/2+X, 3/2-Y, -1/2-Z)
	-	-	2.987(2) ⁴	
1·(p-tol)	3.594(12) ⁵	-	-	(1/2-X, 3/2+Y, 1-Z)
	-	3.590(2) ⁷	-	
	-	-	2.972(5) ⁸	
1·(p-xyl)	3.442(8) ⁹	-	-	(-1+X, +Y, 1+Z)
	-	3.6095(11) ¹⁰	-	(3-X, -1/2+Y, 1-Z)
	-	-	2.897(3) ¹¹	
1·(CHCl ₃)	3.643(10) ¹²	-	-	(1-X, 1-Y, 1-Z)
	-	3.637(2) ¹³	-	(1/2-X, -1/2-Y, 1-Z)
	-	3.528(9) ¹⁴	-	(+X, -1+Y, +Z)

¹C40···Br3, ²C37-H37···π (centroid: C13, C14, C15, C16, C17, C18), ³C007···Br01, ⁴C00A-H00E···π (centroid: C00C, C00B, C00D, C00E, C00F, C00G), ⁵Br1···C7, ⁷Br2···Br3, ⁸C3-H3···π (centroid: C38, C39, C40, C41, C42, C43), ⁹C1···Br3, ¹⁰Br1···Br2, ¹¹C24-H24···π (centroid: C35, C36, C37, C38, C39, C40), ¹²C11···Cl1, ¹³Br1···Br1, ¹⁴Br1···Cl3.

S4. NMR spectral data

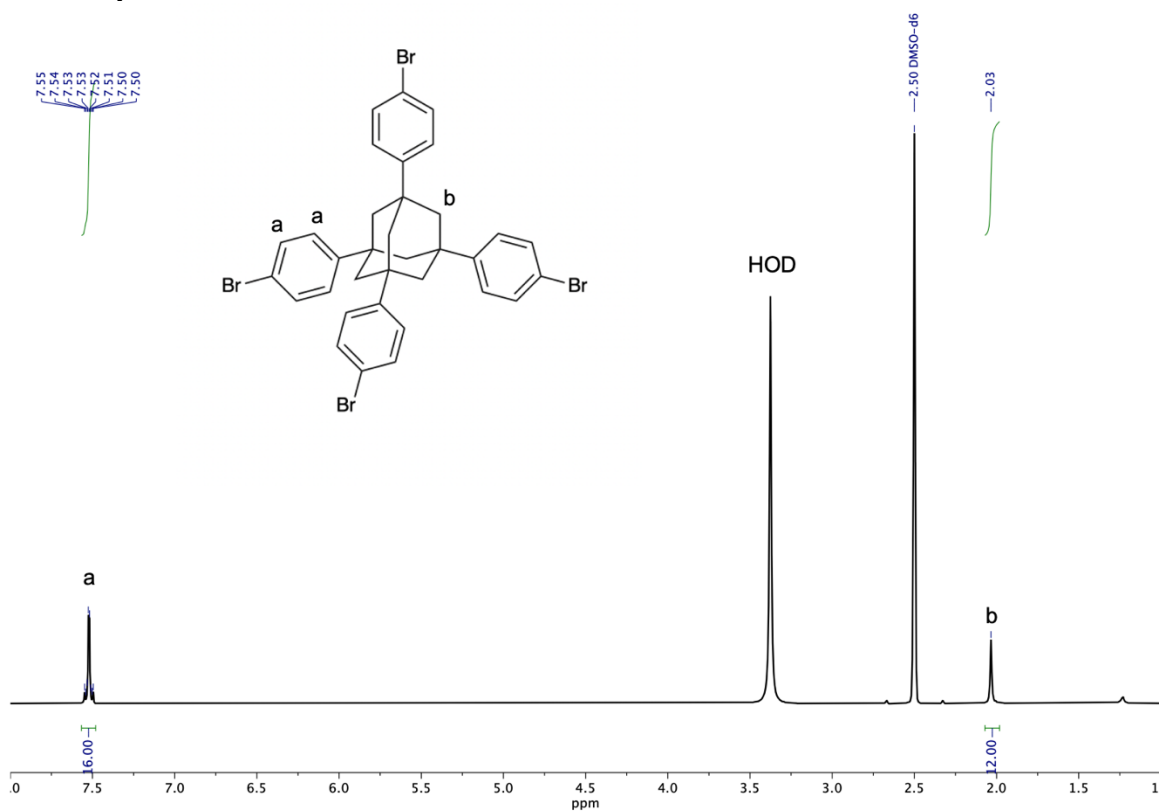


Fig. S4. ^1H NMR spectrum of **apo-1** (400 MHz, DMSO-d_6). We note the ^1H NMR signals display solvent dependency as with similar adamantane systems.⁵

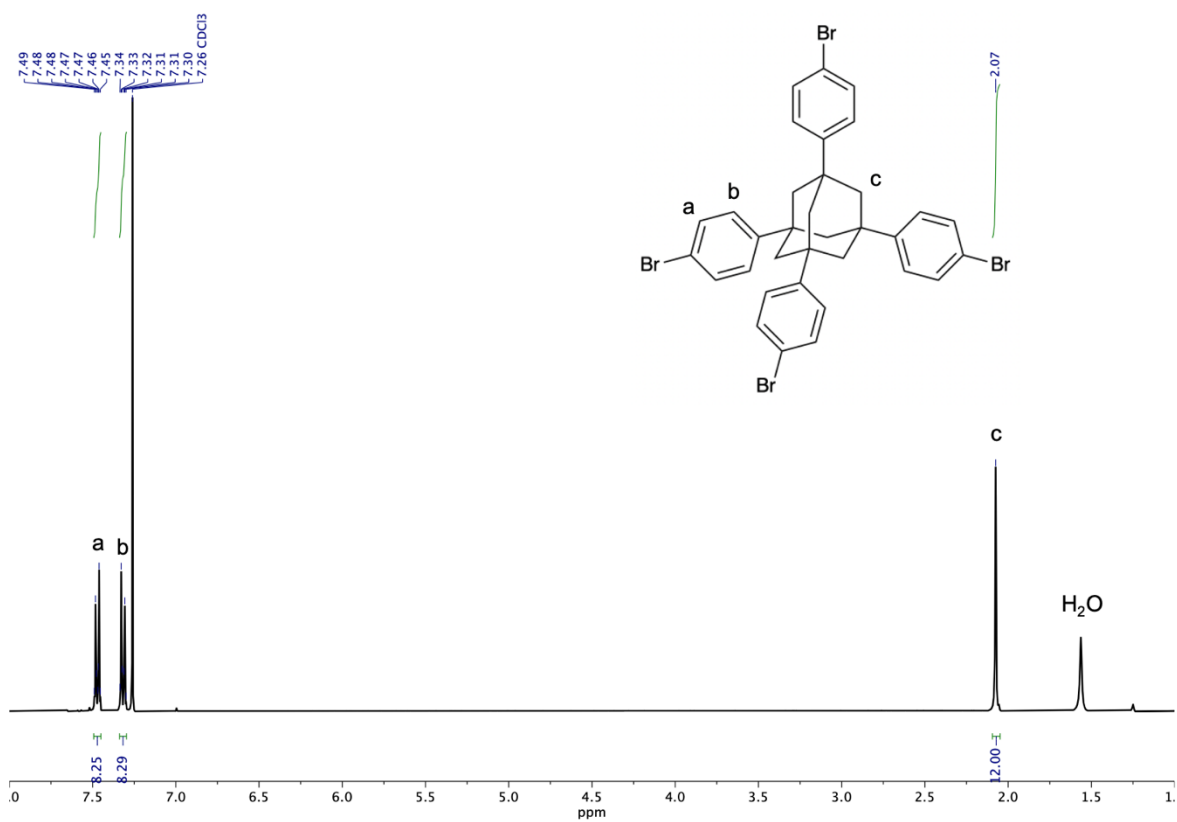


Fig. S5. ^1H NMR spectrum of **apo-1** (400 MHz, CDCl_3). We note the ^1H NMR signals display solvent dependency as with similar adamantane systems.⁵

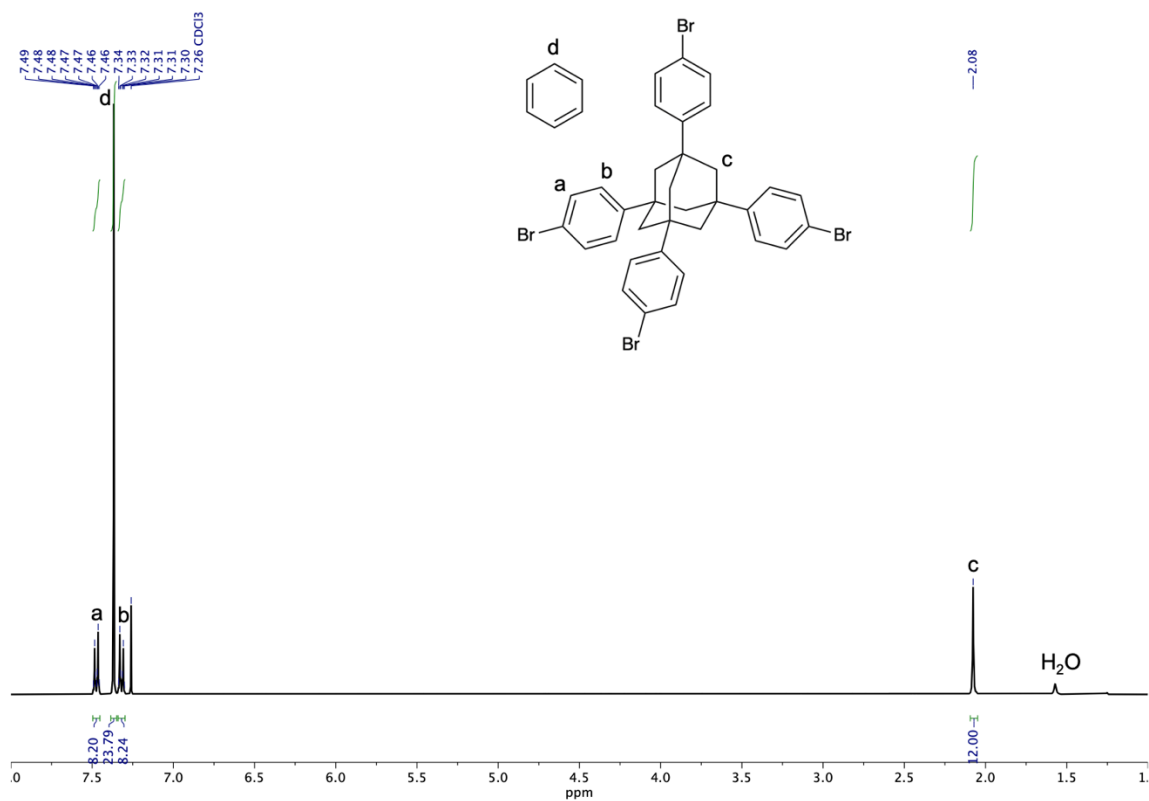


Fig. S6. ¹H NMR spectrum of (1)·(C₆H₆). Integrations show a 4:1 guest to host ratio (400 MHz, CDCl₃). We note the ¹H NMR signals display solvent dependency as with similar adamantane systems.⁵

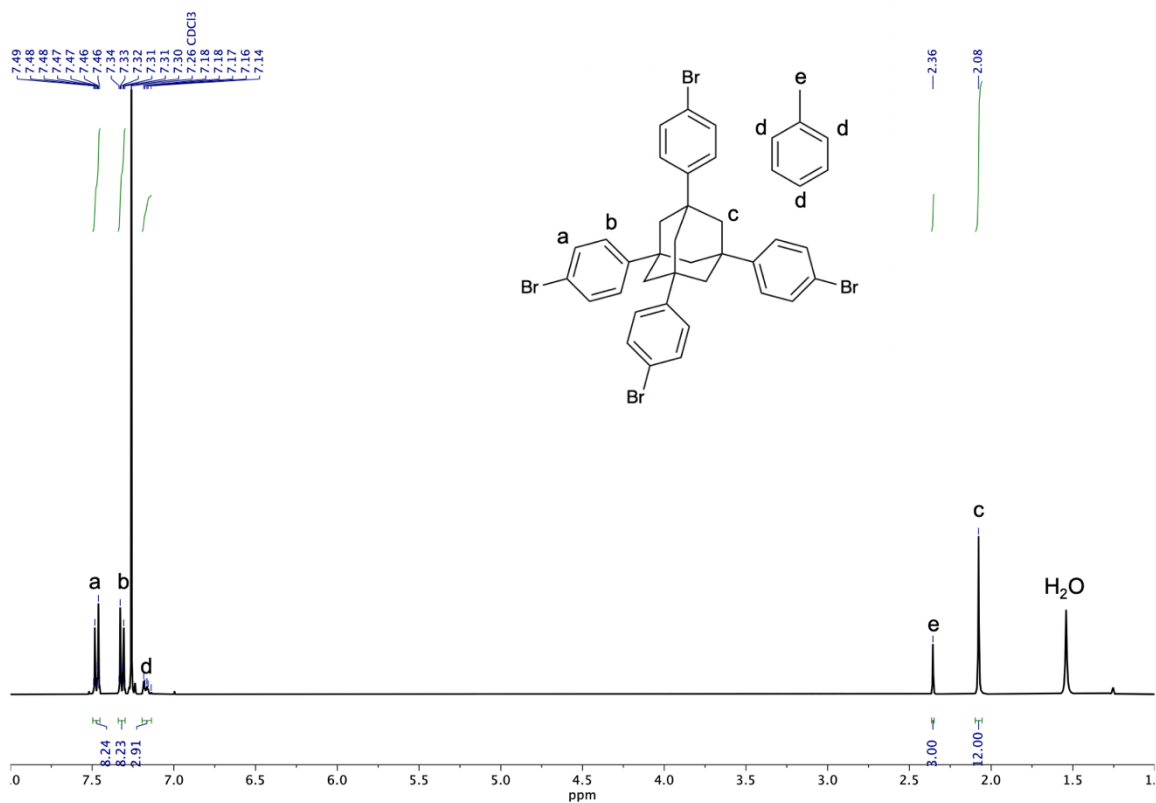


Fig. S7. ¹H NMR spectrum of (1)·(tol). Integrations show a 1:1 guest to host ratio (400 MHz, CDCl₃). We note the ¹H NMR signals display solvent dependency as with similar adamantane systems.⁵

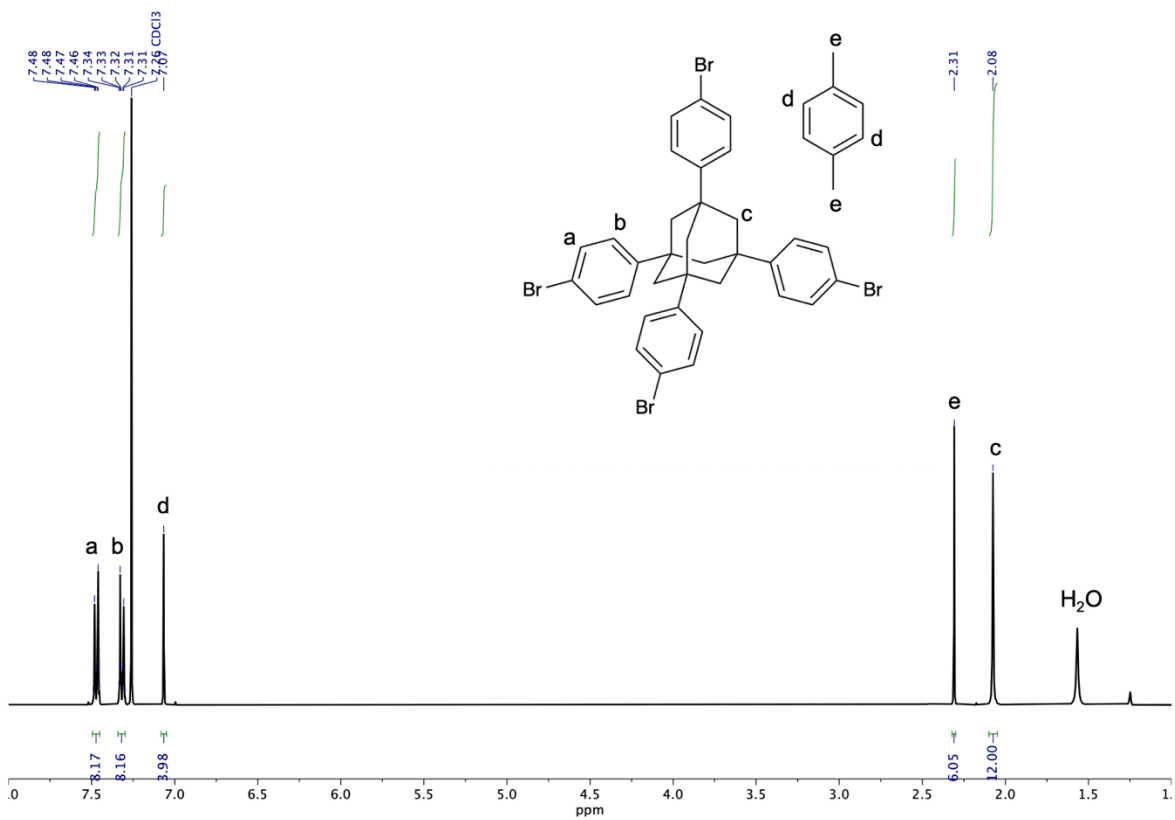


Fig. S8. ¹H NMR spectrum of (1)·(*p*-xyl). Integrations show a 1:1 guest to host ratio (400 MHz, CDCl₃). We note the ¹H NMR signals display solvent dependency as with similar adamantane systems.⁵

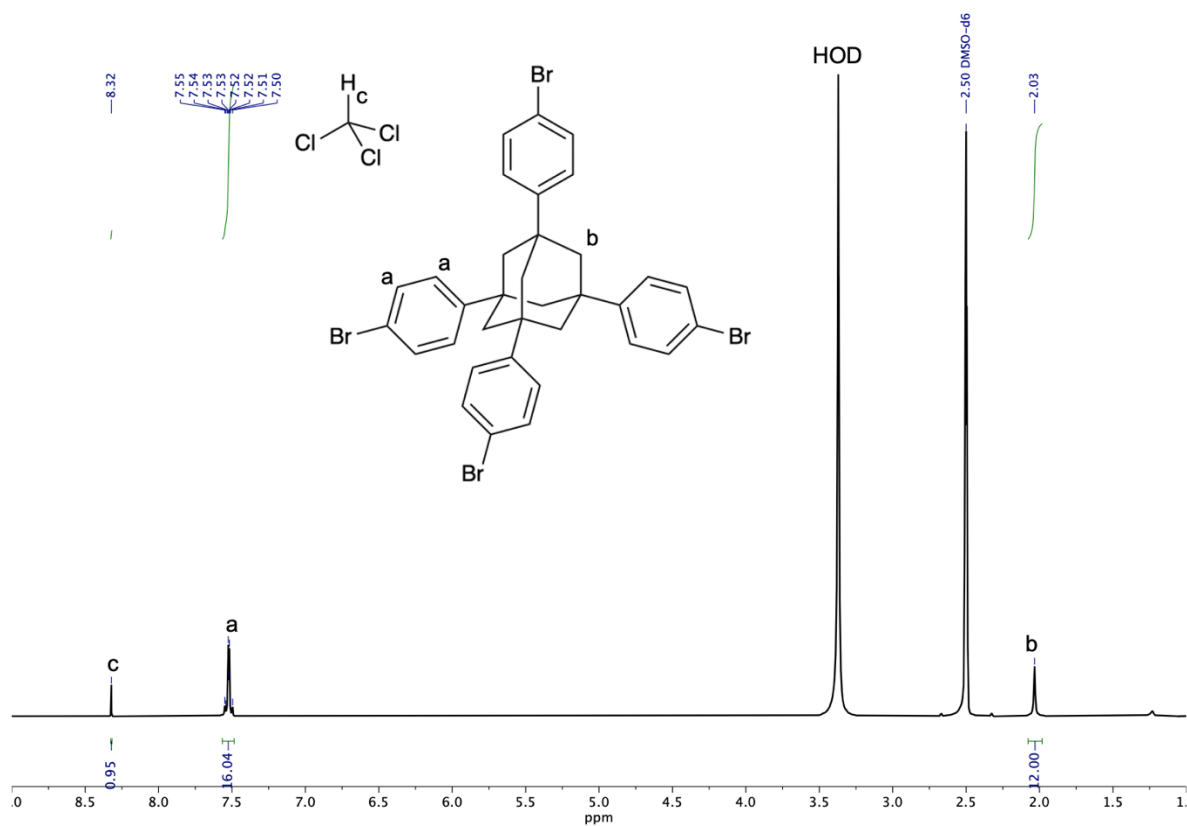


Fig. S9. ¹H NMR spectrum of (1)·(CHCl₃). Integrations show a 1:1 guest to host ratio (400 MHz, DMSO-d₆). We note the ¹H NMR signals display solvent dependency as with similar adamantane systems.⁵

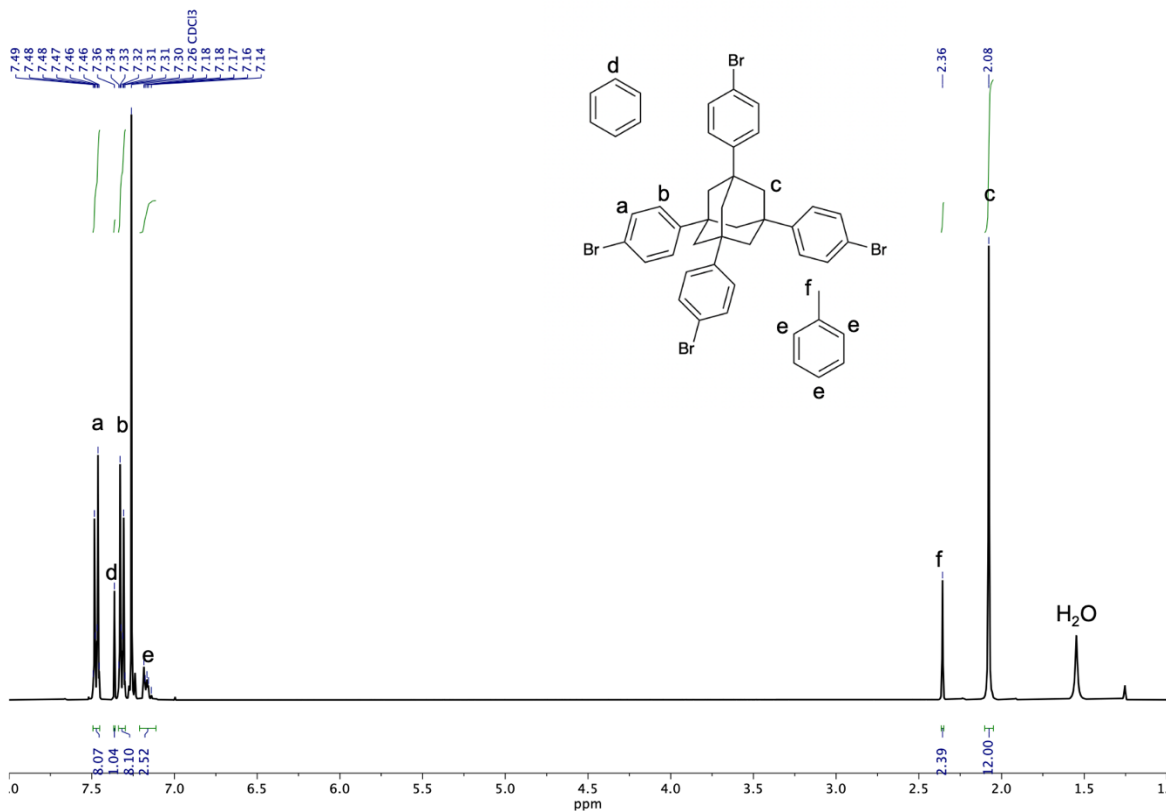


Fig. S10. ¹H NMR spectrum of crystals of **1** grown in a 1:1 mixture of benzene-toluene, resulting in single crystals of **1** with solvent confinement of both. Normalized to adamantane protons. (400 MHz, CDCl₃). We note the ¹H NMR signals display solvent dependency as with similar adamantane systems.⁵

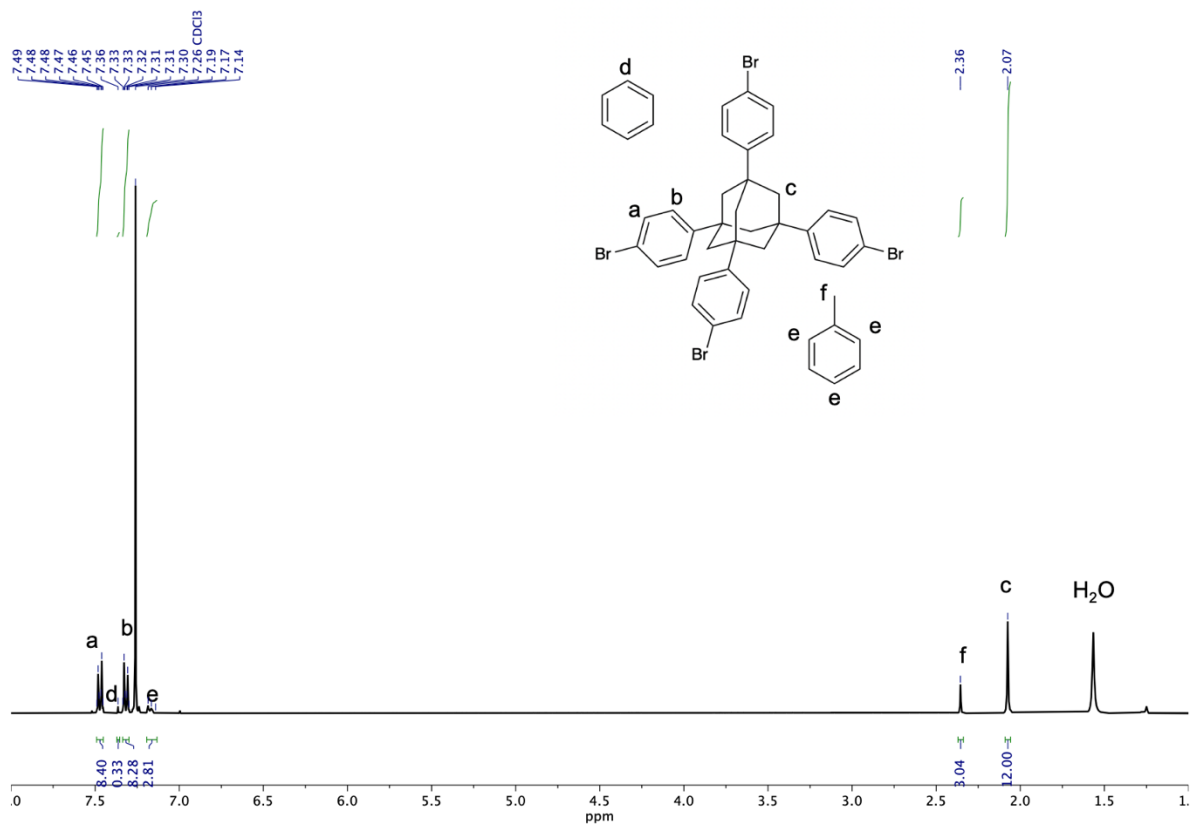


Fig. S11. ¹H NMR spectrum of crystals of **1** grown in a 4.1:0.9 ratio of benzene-toluene, resulting in single crystals of **1** with solvent confinement of both. Normalized to adamantane protons. (400 MHz, CDCl₃). We note the ¹H NMR signals display solvent dependency as with similar adamantane systems.⁵

Table S7. Toluene uptake in comparison to benzene based on ^1H NMR data. Toluene content normalized.

Uptake Number	Relative M(Toluene)	Relative M(Benzene)	Toluene ratio (%)	Benzene ratio (%)
1st	6.00	1.31	82	18
2nd	6.00	0.33	95	5

The relative concentration analysis was carried out using the ^1H NMR signals of H(toluene) (3H of toluene) and H(benzene) (6H of benzene) taken from the single crystals after each uptake with **1**. The signals H(toluene) and H(benzene) were normalized for the number of protons and performed a ratio analysis following the formula:

$$\frac{M(\text{toluene})}{M(\text{benzene})} = \frac{I(\text{toluene})}{I(\text{benz})} \times \frac{N(\text{benz})}{N(\text{toluene})}$$

Where I is the integral, and N is the number of nuclei giving rise to the signal. Since H(toluene) consists of 3H (total H in molecule: 8H) and H(benzene) consists of 6H (total H in molecule: 6H), the equation can be expressed as:

$$\frac{M(\text{toluene})}{M(\text{benzene})} = \frac{I(\text{toluene})}{I(\text{benzene})} \times \frac{6}{3}$$

S5) UNI force field calculations

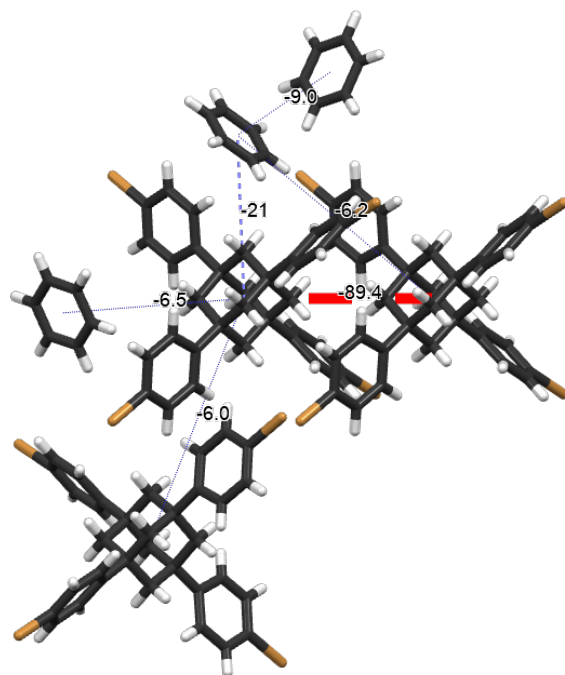


Fig. S12. Intermolecular contacts in **1**·(C₆H₆) using force field potential calculations (UNI) (energies in kJ mol⁻¹). Red indicates the strongest interaction.

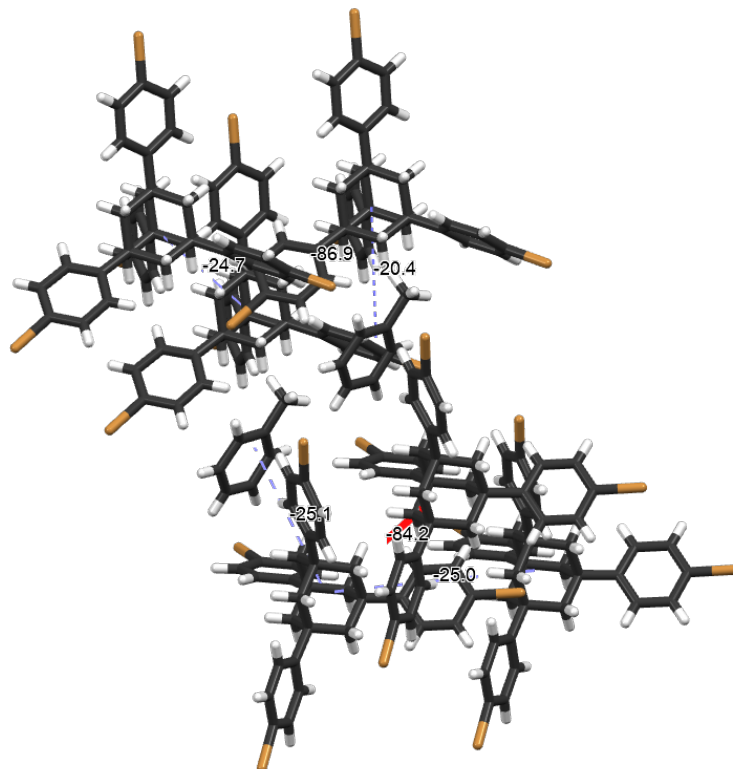


Fig. S13. Intermolecular contacts in **1·(tol)** using force field potential calculations (UNI) (energies in kJ mol⁻¹). Red indicates the strongest interaction.

References

- (1) Sheldrick, G. M. *Acta Cryst. A* **2015**, *71*, 3-8.
- (2) Sheldrick, G. M. *Acta Cryst. C* **2015**, *71*, 3-8.
- (3) Dolomanov, O. V.; Bourhis, L. J.; Gildea, R. J.; Howard, J. A.; Puschmann, H. *J. Appl. Crystallogr.* **2009**, *42*, 339-341.
- (4) Farrugia, L. J. *J. Appl. Crystallogr.* **1999**, *32*, 837-838.
- (5) C. A. Gunawardana, A. S. Sinha, E. W. Reinheimer and C. B. Aakeröy, *Chemistry*, **2020**, *2*, 179-192.